A revisit to the shakedown of pavements under moving surface loads

Jidong Zhao
Department of Civil and Environmental Engineering – Hong Kong University of Science and Technology, Clearwater Bay, Kowloon, Hong Kong

2011 Pan-Am CGS Geotechnical Conference

ABSTRACT
The shakedown of pavements subjected to moving surface loads is investigated in this paper. The pavement is modeled as a half-space Mohr-Coulomb medium. By approximating the sliding and rolling contact between a roller and the half-space road surface by a plane strain trapezoidal load distribution, the shakedown limit is calculated using Melan's static shakedown theorem. We show that many past studies have neglected either or both of the constraints on the residual stress field: the self-equilibrium and the yield condition. The shakedown limits so obtained are normally greater than the true shakedown limit and will be unsafe if used for practical application.

RÉSUMÉ
Nous étudions ici l'adaptation d'un pavage sujet à une charge mobile en surface. Le pavage est représenté par un modèle en demi-espace de Mohr-Coulomb. En faisant appel à une technique d'approximation du contact roulement-glissement entre un rouleau et le pavage en demi-espace par une répartition trapézoïdale des charges sous des conditions de déformation en plan, la limite de l'adaptation est calculée en employant la théorie d'adaptation statique de Melan. Nous montrons que de nombreuses études antérieures ont négligé d'examiner l'une des contraintes sur le champ de contraintes résiduelles ou les deux : l'auto-équilibre et la condition d'écoulement. Les limites de l'adaptation ainsi obtenues sont normalement supérieures à la vraie limite et seront dangereuses en cas d'application pratique.

1 INTRODUCTION

When subjected to cycles of loading, a structure may undergo plastic deformation during the initial applications of the load, but thereafter suffer only elastic strains with no further permanent deformation. This type of behaviour is known as *shakedown*, and the maximum cyclical load at which it occurs is termed as the shakedown limit. The long term behaviour of cohesive-frictional soils under cyclic moving surface loads is important to a wide range of applications in geotechnical and pavement engineering. The performance of pavement road under moving vehicle loads, for example, has been most concerned in pavement design. It is time-consuming and costive, however, to determine the pavement response to successive individual load applications by conducting experiments or by step-by-step calculations as the processes are usually tedious and expensive. Shakedown theory, on the other hand, offers a rational and convenient way to determine the long term load-bearing capacity of the pavements. In particular, the elastic shakedown theorem proposed by Melan (1938) has been proved useful for design purposes in many structural and geotechnical applications. It has been repeatedly applied to the shakedown analysis of a cohesive-frictional half space under moving surface loads (Booker et al., 1985; Collins and Cliffe, 1987; Yu, 2005).

When Melan's theorem is applied to cohesive-frictional materials, however, considerable confusion exists that may give rise to inaccurate and inconsistent predictions of the shakedown limit. Specifically, some of the constraints on the residual stresses that are necessary in deriving rigorous shakedown limits are often inadvertently neglected. This always leads to upper bounds to the static shakedown limit. Two of the commonly found ones include the yield condition and the equilibrium condition on the residual stress. We shall show that the two constraints should be imposed simultaneously with the yield condition on the total stress field, in order for the true shakedown limit to be found. Relaxing either of the two or both will essentially lead to some upper bound (greater) values for the shakedown limit, which, if used for practical application, will lead to unsafe design.

2 SHAKEDOWN ANALYSIS OF PAVEMENT UNDER MOVING SURFACE LOADS

2.1 Approximation on the Rolling and Sliding Contact and Failure Criterion

The pavement can be assumed to be a half space, in which the material is taken isotropic and homogeneous for simplicity. The soil self-weight is assumed small compared to the stress gradient being applied so that it can be safely neglected. It is assumed here the sliding and rolling contact between a vehicle roller and the pavement surface can be approximated by a plane strain trapezoidal contact, as shown below in Figure 1.

If the soil in the half surface is assumed to be isotropic and homogenous, a closed form analytical solution to the elastic stress field under such a trapezoidal contact as shown in Figure 1 has been derived by Zhao et al. (2007). The elastic solution can be used for the shakedown analysis. The Mohr-Coulomb criterion is used to characterize the failure of the pavement material under plain strain conditions:

$$f = \sqrt{\left(\sigma_{zz} - \sigma_{xx}\right)^2 + 4\sigma_{xz}^2} - \left(\sigma_{zz} + \sigma_{xx}\right)\sin\phi - 2c\cos\phi = 0 \quad [1]$$

where c is the cohesion, ϕ is the internal friction angle, and the soil mechanics convention of compression being positive applies.

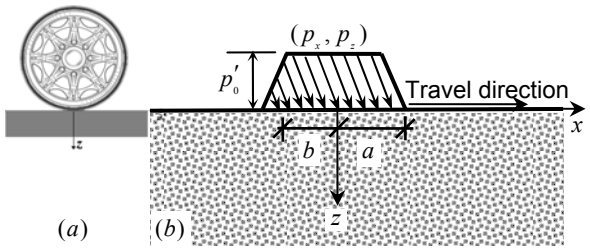

Figure 1. A trapezoidal contact approximation (b) of the pavement surface subject to rolling and sliding load by a vehicle roller (a)

2.2 Application of the Shakedown Theorem and Constraints on the Residual Stress Field

Residual stress is a tension or compression which exists in the bulk of a material without application of an external load, and may be caused by incompatible plastic strains or non-vanishing displacements. For a stable state, the residual stresses present in form of a permanent self-equilibrated stress field that remains in the body after unloading; e.g., after the removal of all external loads and the return of all prescribed surface displacements to zero. In applying Melan's elastic shakedown theorem, it is of pivotal importance to consider two key constraints on the residual stress field: the yielding constraint and the equilibrium condition. Melan's shakedown theorem states that, *a sufficient condition for shakedown to occur is that a time-independent, self-equilibrated, residual stress field can be found such that, when added to the elastic stress field, it produces a combined stress field that nowhere and at no time violates the yield condition*. Therefore, in addition to the requirement that the total stress (elastic stress plus residual stress) field satisfies the yield condition, the residual stress field needs essentially to be elastic and self-balanced too. The three conditions are indispensible in order for the Melan's theorem to be correctly interpreted. Mathematically, we may write the Melan's theorem as the following optimization problem:

$$\lambda_{SD} = \max_{(\lambda,\boldsymbol{\rho})} \lambda \text{ s.t.} \begin{cases} \rho_{ij,j} = 0, \quad n_i \rho_{ij} = 0, \\ f\left(\rho_{ij}\right) \le 0, \\ f\left(\rho_{ij} + \lambda\sigma_{ij}\right) \le 0. \end{cases} \quad [2]$$

where λ is the load factor, ρ_{ij} is a self-equilibrating residual stress field. σ_{ij} is an elastic stress field induced by cyclic external loads. $f(\square)$ is he yield condition. λ_{SD} is the 'static shakedown limit'. For each stage of loading, the sum of the elastic stress and the residual stress, $\hat{\sigma}_{ij} = \rho_{ij} + \sigma_{ij}$, is the total stress or the post transient stress as termed by some others. In Equation 2, the first two equations denote the self-equilibrium conditions on the residual stress field, while the last two inequalities give the yield conditions on the residual stress fields and total stress field, respectively.

As important as they are to the shakedown analysis, relaxing either or both the two constraints on the residual stress may give rise to some interesting implications. Here we consider the following two cases of scenario that may occur with the constraints on residual stress field being missed out: (I) both the equilibrium and yield constraints on the residual stresses are neglected; (II) only the equilibrium condition on the residual stress is neglected. The two cases correspond to the following three optimization problems, respectively:

$$\lambda_I = \max_{(\lambda,\rho_{ij})} \lambda \text{ s.t. } f\left(\rho_{ij} + \lambda\sigma_{ij}\right) \le 0 \quad [3]$$

$$\lambda_{II} = \max_{(\lambda,\rho_{ij})} \lambda \text{ s.t.} \begin{cases} f\left(\rho_{ij}\right) \le 0, \\ f\left(\rho_{ij} + \lambda\sigma_{ij}\right) \le 0 \end{cases} \quad [4]$$

We hereafter call the shakedown load factors obtained by Equations 3 and 4 as type I and type II shakedown limits, respectively.

2.3 Solution Procedures

For the rolling and sliding contact problem, the permanent deformation and residual stress distribution for the plane strain contact will be independent of x and depend only on the depth z. The equilibrium of the residual stresses thus implies that there is only non-zero component ρ_{xx}, which is a function of z only. In view of this, the yield condition on the total stresses for the plane strain half space is:

$$f\left(\lambda\sigma_{ij}, \rho_{xx}\right) = \sqrt{\left(\lambda\sigma_{zz} - \lambda\sigma_{xx} - \rho_{xx}\right)^2 + 4\lambda^2\sigma_{xz}^2} - \left(\lambda\sigma_{zz} + \lambda\sigma_{xx} + \rho_{xx}\right)\sin\phi - 2c\cos\phi = 0 \quad [6]$$

By setting $\partial f / \partial \rho_{xx} = 0$, the following optimal residual stress without any constraint can be obtained:

$$\rho_{xx}^{*} = 2c\tan\phi + \lambda\left(\sigma_{xx} - \frac{1+\sin^2\phi}{\cos^2\phi}\sigma_{zz}\right) \qquad [7]$$

and the corresponding load factor is (see, Collins and Cliffe, 1987; Yu, 2005)

$$\lambda = \frac{c}{|\sigma_{xz}| - \sigma_{zz}\tan\phi} \qquad [8]$$

If, however, the yield constraint on the residual stress is imposed by enforcing $f(\rho_{xx}) = 0$, the following two bounds for ρ_{xx} will be obtained:

$$\begin{cases} \rho_{xx}^{+} = -2c\tan\left(\dfrac{\phi}{2} - \dfrac{\pi}{4}\right) \\ \rho_{xx}^{-} = -2c\tan\left(\dfrac{\phi}{2} + \dfrac{\pi}{4}\right) \end{cases} \qquad [9]$$

where ρ_{xx}^{+} and ρ_{xx}^{-} are the compressive and tensile strength limits of the soil, respectively. The two limits will be used in seeking the shakedown limit below.

In practice, if all conditions as shown in Equation 2 are imposed, it is difficult to reach an analytical solution for the shakedown limit. In this case, we have to resort to numerical solutions. A detailed flow chart for calculating the shakedown limits as well as its various upper bounds has been given by Zhao et al. (2007). A suitable domain around the contact needs to be chosen and be discretized into a fine mesh. The elastic stresses at each nodal point of in the mesh are calculated and are then combined with a critical value of residual stress in the range bounded by Equation 9 to find the minimum value of load factor to be the one affiliated to that node. The process is repeated for all nodal points in the mesh. The static shakedown limit is the maximum load factor among all nodal points. The accuracy of such as solution is governed by the discretisation and additional tolerances. Fine meshes and tight tolerances have to be used to minimise the overall solution error. The contact half-length a, and the cohesion of the soil c, will be used to normalise all other variables. This permits the load factor $\lambda p_0'/c$ to be used to evaluate the shakedown limit and the two upper bounds. Generally speaking, the critical material point for the shakedown load factor occurs within a small distance of the contact area. A domain of width W and depth D around the contact area for consideration should be large enough to cover all possible critical points, while at the same time being as small as possible to reduce the computational effort when a very fine mesh is used (see Figure 2 for a sample mesh). A structured mesh is preferred to an unstructured mesh, as it more convenient for checking the load factor layer by layer.

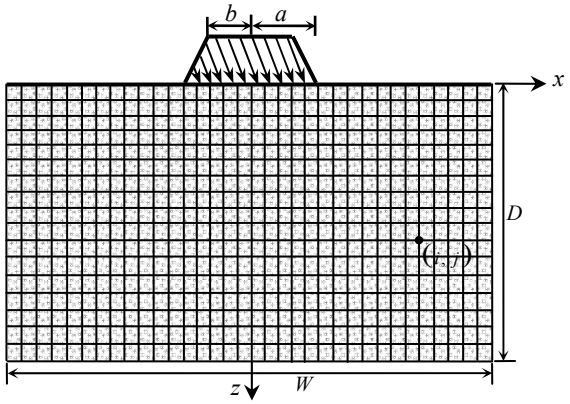

Figure 2. Illustrative mesh used for the shakedown analysis

In the following analysis, we choose a domain of $x = [-1.25a, 1.25a]$ and $z = [0, 1.25a]$, and further partition it into a mesh of 800x400 (in the x and z directions respectively). The number of divisions for checking that the residual stress n_ρ is chosen at a value of 400. The shape of the trapezoid is fixed at $b/a = 0.5$. The friction coefficient μ is assumed to lie in the range of [0, 1]. We investigate four cases of internal frictional angle, $\phi = 0^\circ$, 15°, 30° and 45°.

3 RESULTS AND DISCUSSION

3.1 Shakedown limit and its upper bounds

Presented in Figure 3 are the load factors for shakedown and elastic limit for the chosen four cases of frictional angle. In Table 1 we further summarize the elastic shakedown limits for trapezoidal case in terms of its maximum pressure p_0'. As is observed from Figure 3, the shakedown load factors decrease as the roller friction μ increases, and increase with the increase of internal frictional angle ϕ. If μ is small, the critical position for the shakedown factor is found to be located at subsurface, whereas for cases of large μ, surface failure will be become critical. There is a non-smooth transitional point observed in the curve for static shakedown limit in each case of ϕ which marks the boundary between surface and subsurface failure mechanism for the critical position of shakedown to occur. The value of μ becomes smaller when the internal friction angle increases. This indicates that the surface failure more likely to occur in a frictional soil than less frictional one (or frictionless one).

By neglecting some of the constraints on the residual stress field, it is evident that both type I and type II load factors constitute upper bounds to the static shakedown limit as obtained by Equation 2. And a general trend is observed that $\lambda_E \le \lambda_{SD} \le \lambda_{II} \le \lambda_I$. At small roller friction coefficients when subsurface is critical, the static shakedown limit is identical with the type I and type II upper bounds. When μ becomes greater, the static shakedown limit becomes the smallest of the three and the type I upper bound is the biggest one. Type I and type II upper bounds could be markedly greater than the static shakedown limit (over 80% in some case). Note that these upper bounds have been taken as the shakedown limit in some previous studies. If they are to be used for practical application, it would lead to unsafe design.

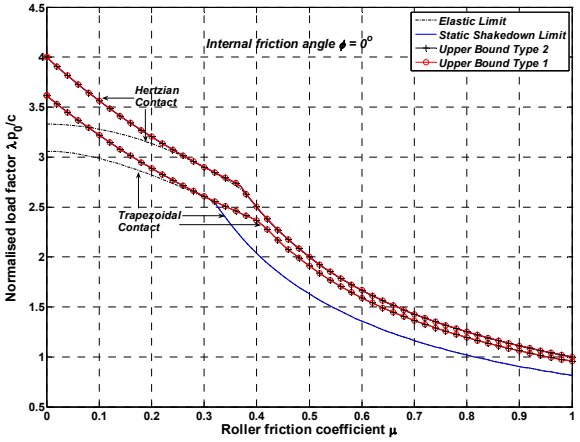

(a)

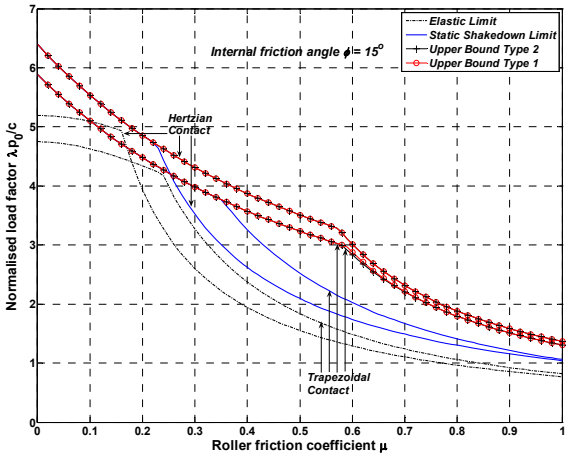

(b)

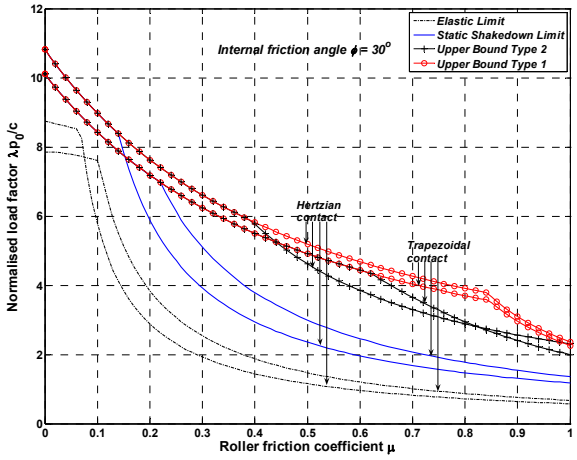

(c)

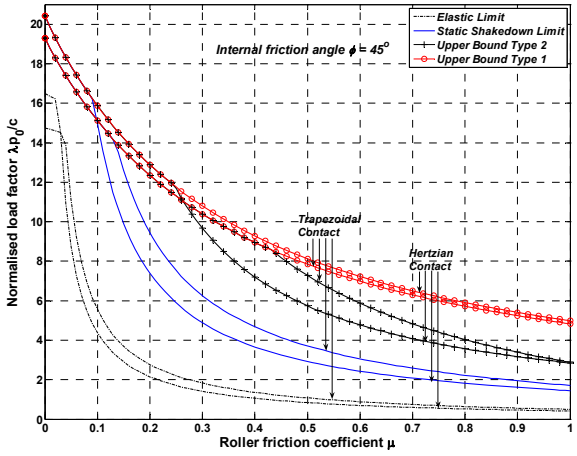

(d)

Figure 3. Load factors for shakedown and elastic limit for an internal frictional angle of (a) $\phi = 0^\circ$; (b) $\phi = 15^\circ$; (c) $\phi = 30^\circ$ and (d) $\phi = 45^\circ$.

Table 1. Shakedown limit for a trapezoidal load distribution with b/a=0.5.

ϕ	$\mu = 0.0$	0.2	0.4	0.6	0.8	1.0
0°	3.789*	3.022*	2.133+	1.422+	1.067+	0.853+
15°	6.164*	4.690*	3.420+	2.123+	1.478+	1.110+
30°	10.588*	7.523*	3.968+	2.576+	1.862+	1.421+
45°	20.193*	9.872+	4.901+	3.210+	2.330+	1.792+

+Surface failure; *Subsurface failure.

We notice similar transitional points in the curves for type I and type II shakedown limits as well. The points occur at a larger value of the roller friction than in the static shakedown limit case. This indicates that a physical realistic residual stress field may cause significant

deformation in the proximity of the surface soil. When combined with an external load that causes larger shear stresses, surface failure will easily be triggered. However, for the cases of type I and type II, relaxing the equilibrium condition and/or the yield constraint on the residual stress may lead to unrealistic soil deformation, e.g., the soil element deforms as a rigid body, such that major portion of the surface load it transmitted to deeper soil elements. This explains why subsurface failure is more often found in the cases of type I and type II at relatively high roller friction. It is this difference in failure mechanism that leads to the difference in the static shakedown limit and the two upper bounds.

3.2 Comparison of the Trapezoidal Case with the Hertzian Contact Approximation

Presented in Figure 3 are also results for Hertzian contact approximation (see Krabbenhøft et al., 2007) for the convenience of comparison with the trapezoidal contact case. To ensure the two cases are comparable, all load factors for the trapezoidal case has been normalised by the maximum pressure p_0 for the Hertzian contact with $b/a = 0.5$. If the trapezoidal maximum pressure p_0' is used for the normalisation, a multiplier of $\pi/3 \approx 1.047$ needs to be applied to the corresponding load factors for the trapezoidal contact case.

At the same contact length and total applied pressure, the static shakedown limit obtained for the trapezoidal contact is found to be smaller than for the Hertzian case for frictionless soils. When the frictional angle of the soil is increased, this trend remains when the roller friction coefficient is small and while subsurface failure is critical. When μ becomes large and surface failure is critical, the trend is reversed. The static shakedown limit for trapezoidal contact case becomes greater. For frictionless soils, the trapezoidal surface pressure distribution under rolling and sliding contact results in a stress field with greater degree of stress concentration. The shakedown limit so derived is thus more conservative. However, for frictional soils, the trapezoidal shakedown limit is less than the Hertzian shakedown limit for cases with small roller friction coefficients, but becomes greater and unconservative when the roller friction coefficient is large.

Meanwhile, we observe that the transitional point that separates the subsurface and surface failure types occurs at smaller μ for Hertzian contact as the internal friction angle is increased. It is not always so in the trapezoidal case. We find for the latter case the transitional point corresponds to $\mu = 0.32,\ 0.35,\ 0.22$ and 0.13 for $\phi = 0^\circ$, 15°, 30° and 45°, respectively. When the soil is frictionless, the transitional value of μ is smaller for the trapezoidal contact case as compared to the Hertzian case, bur larger when the soil is frictional.

3.3 Comparison with Past Results

Figure 4 presents a further comparison of the new shakedown limits obtained in this paper with some previous results. For all four internal friction angles, the new shakedown results for the trapezoidal contact case appear to be close to those obtained by Sharp and Booker (1984), but vary significantly from those given by Collins and Cliffe (1987). The shakedown loads predicted by Collins and Cliffe (1987) are generally smaller than our new results and have no obvious (non-smooth) transition points at all. In addition, the shakedown limits obtained by Yu (2005) clearly are the upper bound type I results in the Hertzian contact case and are generally greater than the true shakedown limits.

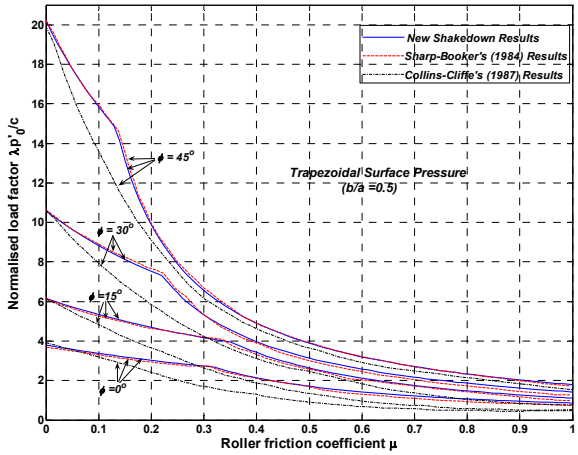

Figure 4. A comparison of the new elastic shakedown limits with those of Sharp and Booker (1984) and Collins and Cliffe (1987).

3.4 Effect of Variable trapezoidal Shape

We have also investigated the effect of the shape of the trapezoidal pressure distribution, governed by the ratio of b/a, on the shakedown load factor. Five values of b/a are selected for this purpose: $b/a = 0, 0.3, 0.5, 0.8, 0.99$. The maximum pressure p_0' and the contact half-length a for the distribution are assumed to be the same for all cases. The computed results, shown in Figure 5, are for a normalised load factor that is scaled for trapezoidal contact by $\lambda p_0'/c$ (not by the maximum Hertzian contact pressure p_0). Note that the case of $b/a = 0$ corresponds to a triangular pressure distribution, while the case of $b/a = 0.99$ approximates the rectangular distribution. The exact rectangular case, where $b/a = 1.0$, cannot be modelled due to the occurrence of a stress singularity at the edge of the contact area due to the tangential traction (see, also, Johnson, 1985).

Figure 5 shows that as b/a is reduced, the shakedown limit increases and the transition from subsurface to surface failure occurs at larger values of μ for the frictional soils considered. Fixing p_0' and a, while varying b/a, corresponds to a roller with a different

overall load. Larger values of b/a generally simulate better the effects of a tyre under higher load ratio. From Figure 5 we also see that when b/a approaches 1.0, the shakedown curve becomes smooth and no obvious transition (non-smooth) point identifying the change from subsurface to surface failure is observed.

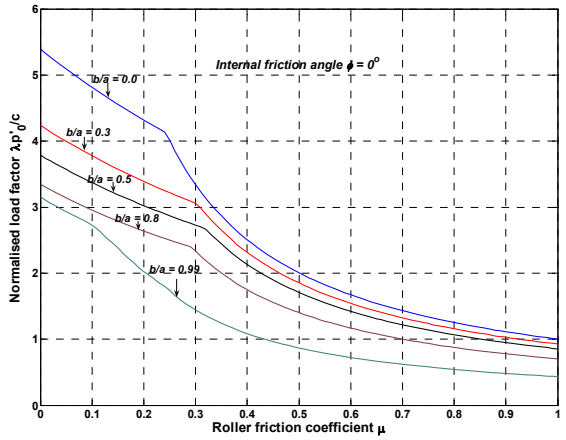

(a)

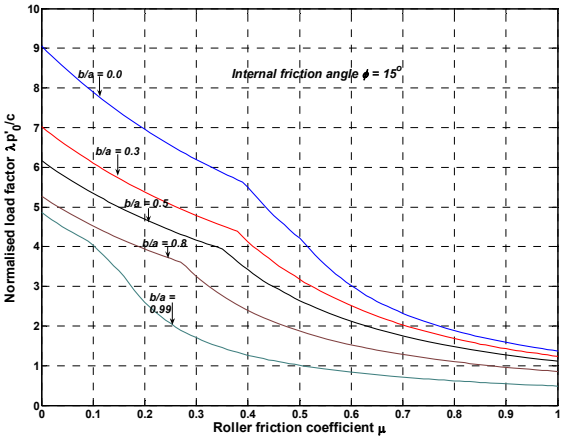

(b)

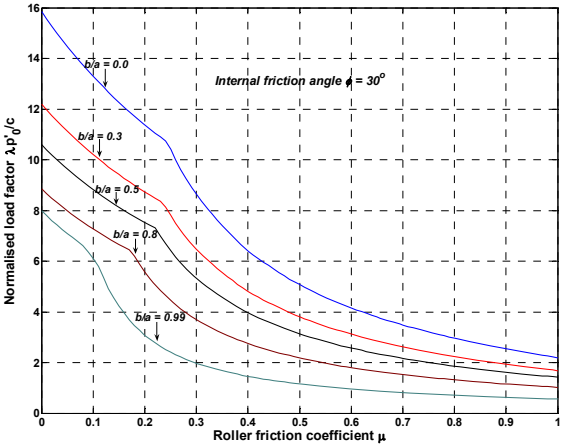

(c)

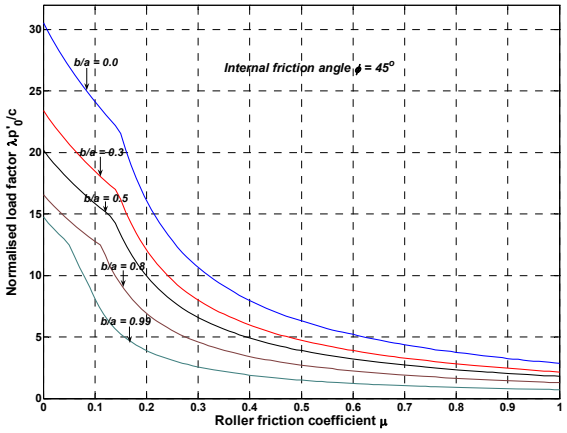

(d)

Figure 5. Variation of static shakedown limit with trapezoidal shape (b/a) at an internal frictional angle of (a) $\phi = 0^\circ$; (b) $\phi = 15^\circ$; (c) $\phi = 30^\circ$ and (d) $\phi = 45^\circ$. The various cases have the same a and the same maximum pressure p_0'. All load factors are normalised by this maximum pressure.

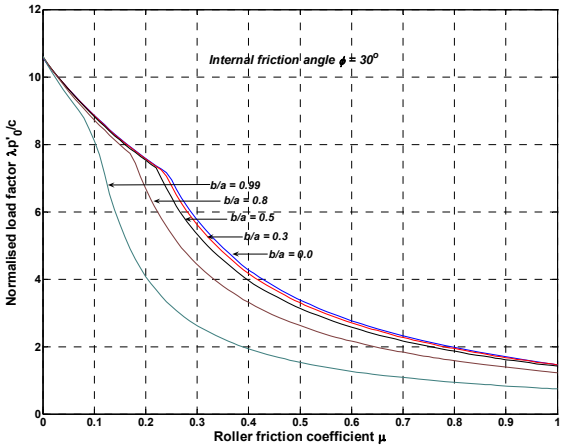

Figure 6. Variation of static shakedown limits to the trapezoidal shape (b/a) for soils with internal friction angle $\phi = 30^\circ$. In this figure, the various b/a with the same a and the same overall load, all the load factors are scaled and normalised by the maximum pressure p_0' for the case $b/a = 0.5$.

Alternatively, we can fix the contact half-length and assume the overall force applied to different trapezoidal distributions is the same. By doing this, we can investigate the cyclic bearing capacity for various contact shapes under the same total load. In this case, the maximum pressure for each case will vary according to b/a. To make the various static shakedown limits for all cases comparable, we use the maximum pressure p_0' for the

case of $b/a = 0.5$ as a benchmark, and normalise all load factors with respect to this pressure and the soil cohesion c. The resulting static shakedown limits are shown in Figure 6. For the same contact length and overall load, the ratio b/a affects the transition from subsurface to surface failure. The larger the ratio b/a is, the earlier this transition occurs in terms of μ.

4 CONCLUSION

Melan's theorem in application to the predictiction of the shakedown limit of a cohesive-frictional half space under moving surface load has been re-examined. It is shown that, other than the yield constraints on the total stresses, the self-equilibrium and yield constraints on the residual stresses are equally indispensable in deriving rigorous lower bound shakedown limit. Otherwise, it will lead to unsafe upper bounds to the true shakedown limits. Comparison of shakedown limits obtained by two approximations for the surface contact loads, the Hertzian contact and trapezoidal contact has been made, as well as with some past studies. The new shakedown limit results derived here will be useful in pavement design as well as in benchmarking shakedown solutions obtained from other numerical methods.

ACKNOWLEDGEMENTS

The work was financially supported by the Research Grants Council of Hong Kong (Project No. 623609).

REFERENCES

Collins, I.F. and Cliffe, P.F., 1987. Shakedown in frictional materials under moving surface loads. *Int. J. Numer. Analy. Meth. Geomech.* 11: 409-420.

Johnson, K. L., 1990. A graphical approach to shakedown in rolling contact. In: *Applied Stress Analysis* (Edited by T. H. Hyde and E. Ollerton). Elsevier, 263-274

Krabbenhøft, K., Lyamin, A.V. and Sloan, S.W., 2007. Shakedown of a cohesive-frictional half-space subjected to rolling and sliding contact. *Int. J. Solids Structures*. 44: 3998-4008.

Melan, E., 1938. Zur plastizität des räumlichenkontinuums. *Ingenieur Archiv* 9: 116-126.

Sharp, R.W. and Booker, J.R., 1984. Shakedown of pavements under moving surface loads. *J. Transportation Engineering*, ASCE 110(1): 1-14.

Yu, H.S., 2005. Three-dimensional analytical solution for shakedown of cohesive-frictional materials under moving surface loads. *Proceedings of the Royal Society A.* 461: 1951-1964.

Zhao, J.D., Sloan, SW., Lyamin, a.V. and Krabbenhøft, K. 2007. Limit Theorems for Gradient-Dependent Elastoplastic Geomaterials. *Int. J. Solids Structures*. 44: 480-506.